

Research Article

Experimental Evaluation of Sulfur Dioxide Absorption in Water Using Structured Packing

Rosa-Hilda Chavez,¹ Nicolas Flores-Alamo,¹ and Javier de J. Guadarrama²

¹Instituto Nacional de Investigaciones Nucleares, La Marquesa, Ocoyoacac, 52750 Mexico City, DF, Mexico

²Instituto Tecnológico de Toluca, Metepec, 52140 México City, DF, Mexico

Correspondence should be addressed to Rosa-Hilda Chavez, rosahilda.chavez@inin.gob.mx

Received 16 December 2011; Revised 5 March 2012; Accepted 4 April 2012

Academic Editor: Diego Gómez-Díaz

Copyright © 2012 Rosa-Hilda Chavez et al. This is an open access article distributed under the Creative Commons Attribution License, which permits unrestricted use, distribution, and reproduction in any medium, provided the original work is properly cited.

An experimental study of hydrodynamic and mass transfer processes was carried out in an absorption column of 0.252 m diameter and 3.5 m of packed bed height developed by Mexican National Institute of Nuclear Research (*ININ* by its acronym in Spanish) of stainless steel gauze corrugated sheet packing by means of SO₂-air-water systems. The experiments results include pressure drop, flows capacity, liquid hold-up, SO₂ composition, and global mass transfer coefficient and mass transfer unit height by mass transfer generalized performance model in order to know the relationship between two-phase countercurrent flow and the geometry of packed bed. Experimental results at loading regimen are reported as well as model predictions. The average deviation between the measured values and the predicted values is $\pm 5\%$ of 48-data-point absorption test. The development of structured packing has allowed greater efficiency of absorption and lower pressure drop to reduce energy consumption. In practice, the designs of equipment containing structured packings are based on approximations of manufacturer recommendations.

1. Introduction

The modelling and study of the beds of structured packing, geometrically ordered, have played scientific and technological challenges, motivated by the urgent need to increase the separation efficiency of separation processes and efficient use of energy and in compliance with environmental legislation [1].

The development of structured packing has allowed greater efficiency of absorption and lower pressure drop to reduce energy consumption [2]. In practice, the designs of equipment containing structured packings are based on approximations of manufacturer recommendations. Conventional structured packing offers the highest efficiency versus other devices. However, it is less resistant to particulate fouling versus grid style packing and there is less experience with conventional packing in this particular service. This is considered a viable option but requires a design that mitigates the potential for particulate fouling [3].

The main feature of the process plant is its large size, handling large quantities of products. These result in specific

problems related to equipment efficiency, energy consumption, and transportation of materials, which affect directly on manufacturing costs.

The high cost per unit volume of the structured packing is a disadvantage [2]; however, economic research in separation processes indicates that they generate a greater contribution to energy savings, so that its design is mainly focused on the reduction of pressure drop per theoretical stage at high-load stages.

The aim of this paper is the experimental evaluation of sulfur dioxide absorption in water with high-efficiency packings, manufactured at the Mexican National Institute of Nuclear Research (*ININ*), and operation behavior based on hydrodynamic and mass transfer models. These models describe fluid dynamic relationship in packed columns with countercurrent flow of gas and liquid phases [4–6]. The Billet model was made by considering void fraction in bed of packing of multiplicity of vertical channels through which the liquid flows downwards in the form of a film countercurrent to the ascending gas stream.

2. Materials and Methods

The methodology was divided in two parts: (i) the use of hydrodynamic and mass transfer models to determine the column diameter and height, respectively, and (ii) the use of other packing, as liquid-gas contactor, in order to determine the absorption column dimensions, one manufactured at the *ININ* and the other by *Sulzer Brothers Limited*.

2.1. Hydrodynamic Behavior and Mass Transfer Models.

Equations that were known for calculating mass transfer process during two-phase countercurrent flows in packed columns were those that apply to the range extending up to the loading points. At loading regimen, the shear stress in gas stream supports an increasing quantity of liquid in the column, with the result that the liquid hold-up greatly increases. At flooding points, the liquid accumulates to such an extent that column instability occurs. Mass transfer in this upper loading regimen can be described if these fluid dynamic relationships are taken into consideration [4–6]. The equations take due account of geometric, hydrodynamic and system-related parameters that they govern the fluidity behavior and mass transfer [4–6]. The fluid dynamics and mass transfer description take into account the great diversity in the geometry, structure and materials for packings in industrial columns, which normally entails differences in the fluid dynamics under operation conditions and thus in the packing performance. Mass transfer calculation allows for the continuous decrease in the average effective liquid load at gas velocities above the loading point.

2.2. Hydrodynamic Model for Hazardous and Structured Packings. The pressure drop per unit packed height $\Delta P/H$, the liquid hold-up $h_{L,S}$ and the model flow factor ξ_S [4–6] have been used for the packed columns prediction. The load point is described by (1):

$$h_L = 4.5803 \left(\frac{Re_L}{Fr} \right)^{0.3507},$$

$$\frac{\Delta P}{H} = \xi_L \left(\frac{a_g}{2} + \frac{2}{d_s} \right) \frac{1}{(\varepsilon - h_L)^3} u_V^2 \rho_V, \quad (1)$$

$$\xi_L = 0.45 W \left(\frac{64}{Re_V} + \frac{3}{Re_V^{0.9}} \right) \left(\frac{\varepsilon - h_L}{\varepsilon} \right)^{(3-x)},$$

where Re_L and Re_V are the *Reynolds* numbers for the liquid and gas phases film flow, respectively, Fr is the *Froude* number, ξ_L is the resistance coefficient, a_g is the geometric packing area (m^2/m^3), d_s is the column diameter (m), ε is the void fraction (m^3/m^3), u_V is the superficial vapor velocity (m/s), ρ_V is the gas (or vapor) density (kg/m^3), C_P and x are constants determined from experiment data, and W is the wetting function.

2.3. Mass Transfer Model for Structured Packing. The two-resistance model [4–6] is used with the assumption of thermodynamic equilibrium at the phase interface. This is useful for either rate-based or equilibrium stage-based computational routines. It is assumed that the mass transfer follows

the laws of stationary diffusion valid for short periods of contact between the phases involved and is described by the following relation, formulated by *Higbie*. The basic parameters of the model are the gas (or vapor) and liquid phases mass transfer coefficients β_V and β_L , respectively, and the effective interfacial area a_{Ph} :

$$\beta_V a_{Ph} = 1.02 F_V^{3.5} u_L^{-2.15} D_V^{0.67},$$

$$\beta_L a_{Ph} = \frac{u_L}{HTU_L} = C_L \left(\frac{\rho_L g}{\eta_L} \right)^{1/6} \left(\frac{D_L}{l_\tau} \right)^{1/2} a_g^{2/3} u_L^{1/3} \left(\frac{a_{Ph}}{a_g} \right),$$

$$\frac{a_{Ph}}{a_g} = 1.5 (a_g d_h)^{-0.5} \left(\frac{u_L d_h}{\nu_L} \right)^{-0.2} \left(\frac{u_L^2 \rho_L d_h}{\sigma_L} \right)^{0.75} \left(\frac{u_L^2}{g d_h} \right)^{-0.45}. \quad (2)$$

The quantity a_g is the geometric packing area (m^2/m^3); $\beta_V a_{Ph}$ and $\beta_L a_{Ph}$ the gas and liquid phase (1/h) volumetric mass transfer coefficient, respectively; u_L the liquid load, (m^3/m^2s); d_h the hydraulic diameter of the packing (m); η_L the dynamic viscosity (kg/ms); σ_L the surface tension; g the gravitational constant, 9.8 m/s^2 ; ν_L the cinematic viscosity (m^2/s); D_L the liquid phase, (m^2/s) solute diffusivity; C_L a constant determined from experiment data; l_τ the characteristic length of the path of contact.

The two-film model is based on the number of gas and liquid resistance transfer global units ($NTUs$) that are related to the mass transfer efficiency in terms of the height of a mass transfer global unit (HTU) [7–9].

The packed total column height Z for the gas and liquid is:

$$Z_G = HTU_{OG} * NTU_{OG},$$

$$Z_L = HTU_{OL} * NTU_{OL}. \quad (3)$$

The application of the two-film model is frequently used to relate the height of the transfer global unit (HTU_{OG} or HTU_{OL}) to the height of the gas HTU_G and liquid HTU_L transfer units to the absorption:

$$HTU_{OG} = HTU_G + \lambda HTU_L,$$

$$HTU_{OL} = HTU_L + \frac{1}{\lambda} HTU_G, \quad (4)$$

The height of the transfer global units is determined by (5):

$$HTU_{OV} = HTU_V + \lambda NTU_L = \frac{u_V}{\beta_V a_{Ph}} + \left(\frac{m}{L/V} \right) \frac{u_L}{\beta_V a_{Ph}}. \quad (5)$$

The quality λ is given by

$$\lambda = m \frac{V}{L}, \quad (6)$$

where m is the ratio of the slope of the equilibrium line to the operation line, and (L/V) is known as the removed factor. The absorption factor is the inverse of λ .

2.4. Absorption Column. Countercurrent contact in a structured packed column of the lean solvent with the process gas transfers the SO_2 to the liquid, producing the rich solvent and a cleaned gas. All the constants or adjusted parameters were determined by the experiments data reported in this work, by using an absorption column measured 3.37 m and 0.252 m internal diameter packed, with stainless steel gauze corrugated sheet packing, named *ININ18*, by means of SO_2 -air-water systems. The packed bed height was 2.52 m. The column has 6 *Lucite* peeholes of 0.0127 m thick and 0.152 m diameter, arranged in pairs on the body of the column to display the liquid and gas flow inside. The packing is supported by a stainless steel ring. The fluid flow is evenly distributed over the surface of the packing through a distributor plate built in stainless steel, 16-gauge stainless steel tube 0.0254 m diameter, schedule 40, constructed to

allow the stability of the forces between the fluids inside the column. The dispenser leaves a free space within the column, 33%, for the passage of gas flow.

The tubing for the inlet and outlet of liquid and gas flows is of carbon steel, schedule 40, and has a diameter of 0.0254 m. The supply pipe SO_2 is stainless steel and has a diameter of 0.0127 m. There is also a storage tank ST (see Figure 1), the liquid flow outlet port, and two sampling input and output of the gas flow, SP1 and SP2, respectively. Monitoring of changes in fluid temperature along the packed bed was carried out with 6 thermocouples type J: TI1, TI2, TI3, TI4, TI5 and TI6, as shown in Figure 1. Air is fed with a pair of parallel compressors BC1 and BC2, *D'vilbis* marks 5 HP, and *Twistair* power of 20 HP, obtaining a maximum flow of 0053 m^3/s of air. The pressure drop caused by the air flow through the packed bed was recorded with the differential pressure meter ΔPI2 .

The number of units overall mass transfer to the gas side, NTU_{ov} , was determined by (3):

$$NTU_{ov} = \int_{y_{in}}^{y_{out}} \frac{dy}{y^* - y} = \frac{y_{out} - y_{in}}{((y_{out}^* - y_{out}) - (y_{in}^* - y_{in})) / (\ln((y_{out}^* - y_{out}) / (y_{in}^* - y_{in})))}, \quad (7)$$

where y_{in} and y_{out} are the concentrations of SO_2 at inlet and outlet gas stream, respectively, and $*$ is concentration of SO_2 in equilibrium.

2.5. Use of Different Packings. Table 1 shows the geometric characteristics of the two structured packings, where α is the corrugated angle with respect to vertical axis of the column, n_t is the gauze threads number per square foot, B is the long of the channel flow, S is the side corrugated wide, θ is the corrugated angle, ρ_p is the packing density, ε is the void fraction, and a_g is the geometric area of the packing.

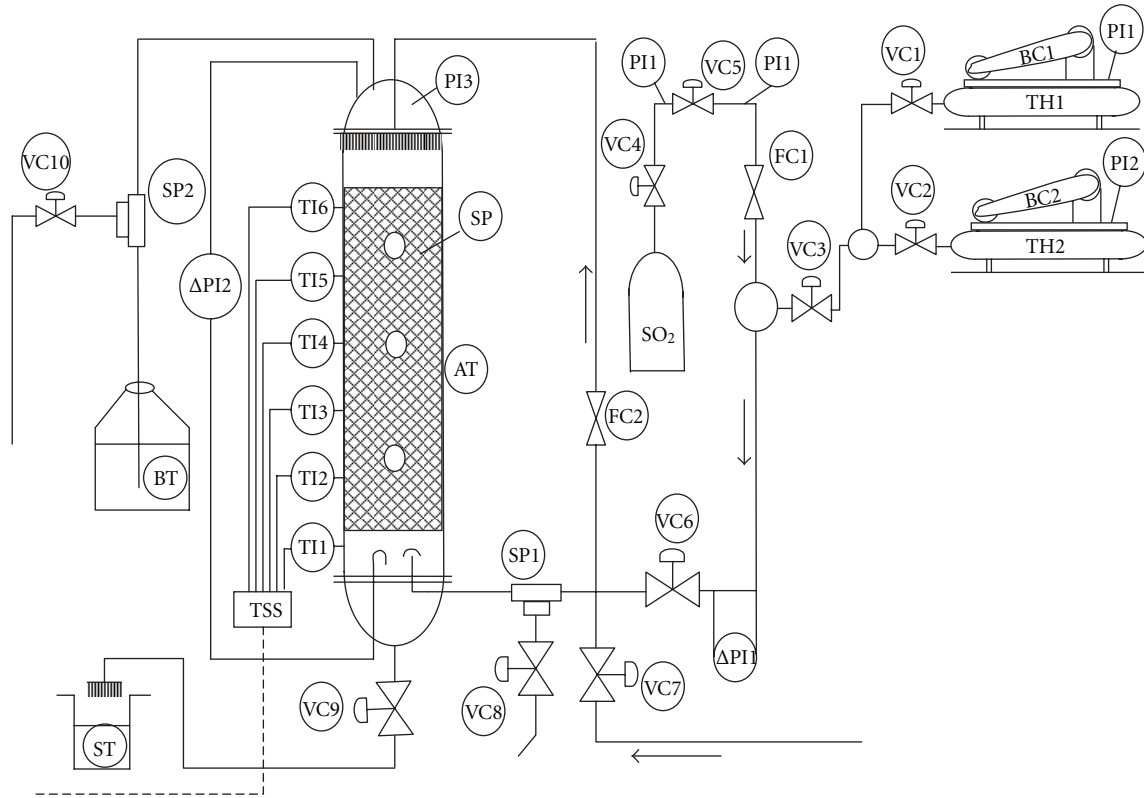
3. Results and Discussion

The mass transfer results and $\%Re_c$ are the recuperation percentages like SO_2 absorbed or removed in the water presented in Table 3. Table 2 shows experimental data, where y_{in} and y_{out} are the inlet and outlet mol fraction concentration, respectively, and the SO_2 concentrations were determined by chromatography analysis. The experiments were conducted to loads less than 70% of flood; in this case the resistance to mass transfer is located in gas phase. Equations allow the determination of the quantities, on the basis of which are the efficiencies of the test system. Furthermore the research can be applied for absorption system.

Figure 2 shows the liquid hold-up with respect to the gas capacity factor F_V . If the gas velocity is larger than $u_V = u_{V,S}$, the liquid hold-up increases rapidly above the value at the loading point, that is, $h_L > h_{L,S}$ until the flood point is reached, that is, $h_L = h_{L,FI}$. At this point, all the liquid is

forced upwards by the stream of gas in the bed. The liquid hold-up of *ININ18* is greater than that of *Sulzer BX* by 44 to 63%, depending upon the values of α , B , S , ε , and a_g . This percentage variation depends on the operation regimen. The angle of inclination of the flow channels α of *ININ18* is lower compared to the *Sulzer BX*; this causes the residence time of liquid phase is greater than the second packing. Figure 3 shows the pressure drop per unit packed height with respect to the gas capacity factor, from 49 to 84.5 $\text{m}^3/\text{m}^2\text{h}$ of liquid velocity. The *Sulzer BX* pressure drop per unit packed height is less than *ININ 18* packing. This result is a consequence of their geometry parameters. The *Sulzer BX* has its maximum flow capacity of 0.83 $\text{kg}^{1/2} \cdot \text{m}^{-1/2} \cdot \text{s}^{-1}$ (0.927215 m/s) and the *ININ18* at 1.4369 $\text{kg}^{1/2} \cdot \text{m}^{-1/2} \cdot \text{s}^{-1}$ (1.6051 m/s), which is attributed to the difference in the diameter of the columns used, corresponding to 0.07 m and 0.252 m, respectively. *Sulzer BX* packing generates lower pressure drop compared to *ININ18*. Figure 3 shows liquid flow at $U_L = 84.5$ and $82.34 \text{ m}^3/\text{m}^2 \cdot \text{s}$, loading zone *ININ18* at $F_V = 0.85 \text{ kg}^{1/2} \cdot \text{m}^{-1/2} \cdot \text{s}^{-1}$ ($U_V = 0.9495 \text{ m}^3/\text{m}^2 \cdot \text{s}$), and flooding at $1.3 \text{ kg}^{1/2} \cdot \text{m}^{-1/2} \cdot \text{s}^{-1}$ ($U_V = 1.45226 \text{ m}^3/\text{m}^2 \cdot \text{s}$), while *Sulzer BX* loading zone at $F_V = 0.62 \text{ kg}^{1/2} \cdot \text{m}^{-1/2} \cdot \text{s}^{-1}$ ($U_L = 0.6926 \text{ m}^3/\text{m}^2 \cdot \text{s}$) and flooding at $F_V = 0.93 \text{ kg}^{1/2} \cdot \text{m}^{-1/2} \cdot \text{s}^{-1}$ ($U_L = 1.0389 \text{ m}^3/\text{m}^2 \cdot \text{s}$). Although the pressure drop *ININ 18* is greater than that of *Sulzer BX*, this is not as great as conventional random packings. It is expected that the greater capacity of operation of *ININ18* is dependent on the geometry of the packing, the porosity, and diameter of column.

Figure 4 shows the volumetric mass transfer coefficient, of *ININ18* packing, with respect to the gas capacity factor,



AT	Absorption column	PI	Pressure meter
T	Temperature	SP1	Sample port
BC	Compressor	FC	Flow controller
BT	Bubble tank	SP	Structured packing
ST	Storage tank	TSS	Temperature sensor selection
TH	Compressor tank	SO ₂	SO ₂ tank
VC	Control valve		

FIGURE 1: Experimental absorption process.

TABLE 1: Geometric characteristic of structured packing.

Packing material	Stainless steel		Units
	ININ18	Sulzer BX	
α	35	30	°
n_t	36	60	
B	0.0165	0.012	m
S	0.012	0.009	m
θ	45	45	°
ρ_p	317.1	187.52	kg/m ³
ε	0.9633	0.90	
a_g	418	498	m ² /m ³

TABLE 2: Experimental data.

$u_L \left[\frac{\text{m}^3}{\text{m}^2 \cdot \text{s}} \right]$	$u_V \left[\frac{\text{m}^3}{\text{m}^2 \cdot \text{s}} \right]$	$F_V \left[\frac{\text{kg}^{1/2}}{\text{m}^{1/2} \cdot \text{s}} \right]$	$y_{in} 10^{-2}$	$y_{out} 10^{-2}$
0.01361	0.621925	0.55954	0.868	2.627
0.01361	0.813622	0.73201	0.868	2.627
0.01361	1.005318	0.90449	0.868	9.292
0.01832	0.621925	0.55954	1.134	3.442
0.018325	0.809129	0.72797	1.134	3.442
0.01832	0.996333	0.89640	1.134	3.442
0.023477	0.621925	0.55954	1.203	1.217
0.02347	0.818114	0.73606	1.203	1.217
0.02347	1.014304	0.91257	1.203	1.217

whereas Figure 5 presents the global mass transfer unit height with respect to the gas capacity factor. Both graphs show the experimental data as well as the tendency predicted from

Billet model [4–6] and equivalent behavior for other mass transfer system [7, 10]. The average deviation between the measured and predicted values is $\pm 5\%$.

TABLE 3: Mass transfer results.

NTU_{OV}	HTU_{OV} [m]	$\beta_V a_{ph}$	% Re_c
3.9048	0.6453	0.98	97
6.5625	0.3839	2.15	97
12.976	0.1942	5.26	89
3.4196	0.7369	0.85	97
4.3123	0.5843	1.40	97
6.026	0.4182	2.42	97
3.378	0.7459	0.84	99
3.933	0.6407	1.29	99
4.823	0.5225	1.94	99

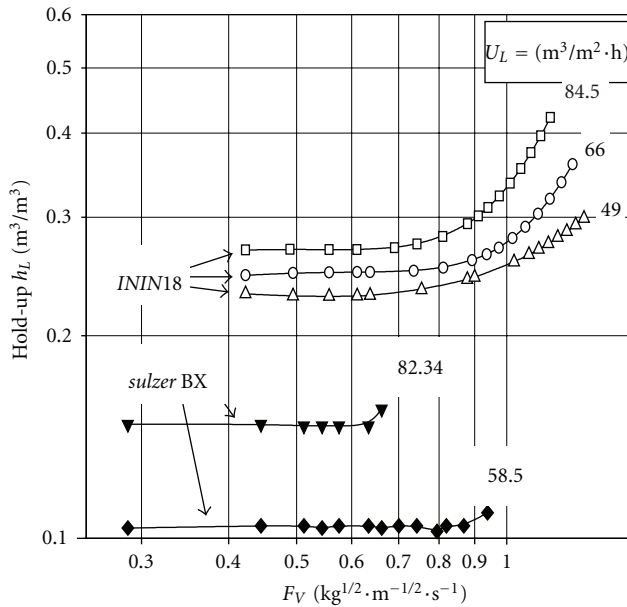


FIGURE 2: Liquid hold-up versus the gas capacity factor.

Figure 5 shows the trend of lower height per unit of mass transfer, when the gas flow increases. This is the result of the mass transfer efficiency increases with increasing gas flow (Figure 4), promoting the formation of the uniform liquid film on the entire surface of the packing and that the flow channel is sufficiently large to allow a homogeneous mixed phases.

This paper highlights the benefit of identifying and evaluating pressure drop in a SO₂-air-water system; this new way of using existing models can complement the assessments made in an equivalent system as developed by Kuntz and Aroonwilas, [7]; Aroonwilas et al., [10] in the CO₂ absorption using MEA, in which they determined mass transfer coefficients through the use of processes, which, although different, are found to be comparable to the process discussed in this paper by trends in the parameters under study.

4. Conclusions

- (i) The *ININ18* packing was higher capacity and lower geometric area than *Sulzer BX*, due to the type

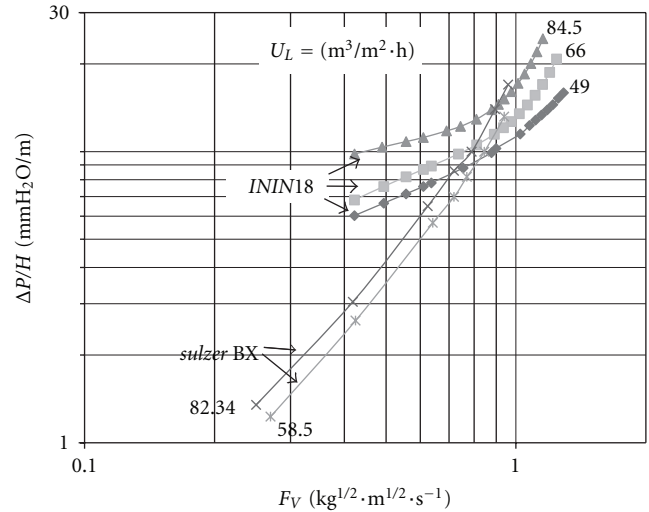


FIGURE 3: Pressure drop versus the gas capacity factor.

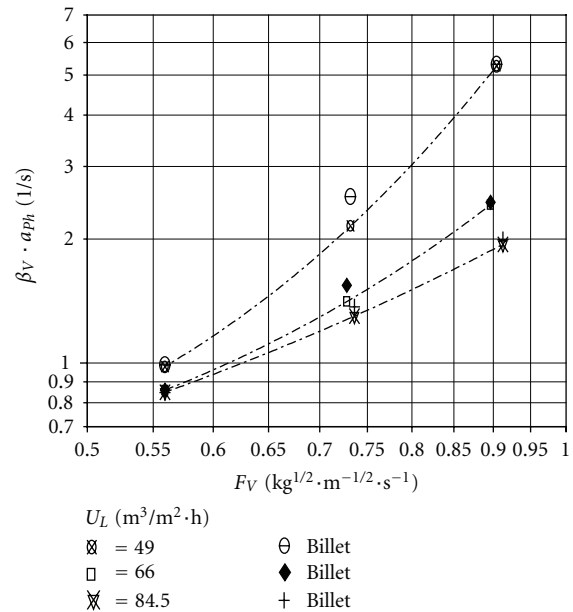


FIGURE 4: Global mass transfer coefficient versus the gas capacity factor.

of mesh they were built with, with 18 mesh and 60 mesh, respectively.

- (ii) *ININ18* packing allowed better distribution of liquid than the *Sulzer BX* packing on the surface and larger residence time of the liquid on the surface of the packing, as a result of a greater angle of the flow channel about the vertical axis of the column, which increases the separation efficiency.

- (iii) The *ININ18* packing liquid hold-up was higher than *Sulzer BX* packing, as a result of the flow channel angle α , even though the flow channel dimensions and porosity of the last one are lower.

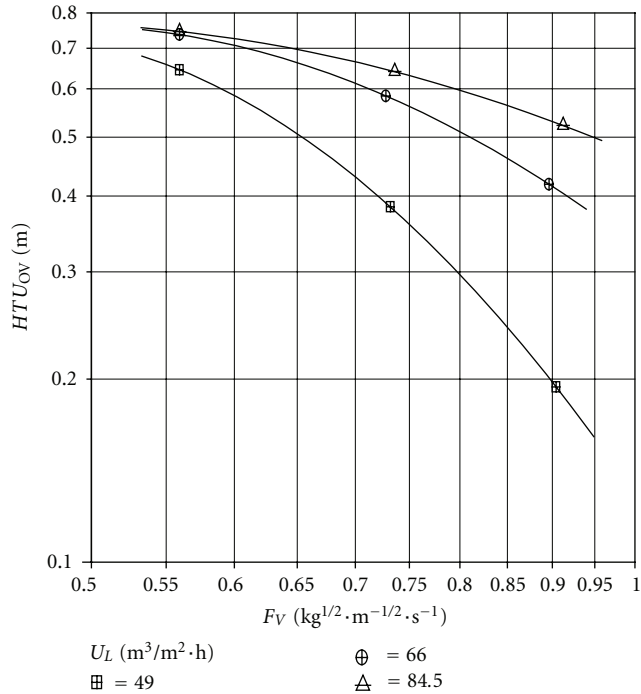


FIGURE 5: Global height mass transfer unit versus the gas capacity factor.

(iv) The pressure drop $\Delta P/H$ generated by the packing *ININ18* was greater than the *Sulzer BX* due to increased liquid hold up h_L .

(v) *ININ18* packing efficiency was high performance, since the removal of SO_2 was obtained, of the gaseous mixture from 97 to 98%. The lower height of a mass transfer unit by the gas side is achieved at higher gas flow.

Acknowledgment

Financial support of this work was provided by Consejo Nacional de Ciencia y Tecnología (CONACyT), Project nos: EDOMEX-C02-2009-135728 and SEP-CONACyT-CB-2007-01-82987.

References

- [1] F. Rong, Y. Lan, S. Zeng, and H. Yu, "Waste energy recovery CDM projects in China: status, challenges and suggestions," *Climate Policy*, vol. 12, pp. 98–114, 2012.
- [2] M. Haghshenas, M. H. Fard, M. Zivdar et al., "CFD simulation of mass transfer efficiency and pressure drop in a structured packed distillation column," *Chemical Engineering and Technology*, vol. 30, no. 7, pp. 854–861, 2007.
- [3] D. K. Stevens and M. R. Tonjes, "Review of CANSOLV SO_2 scrubbing system first commercial operations and application in the oil and gas industry," in *Proceedings of the 54th Annual Laurance Reid Gas Conditioning Conference*, Form no: 170-01463-0904, 2004.

- [4] R. Billet and M. Schultes, "Fluid dynamics and mass transfer in the total capacity range of packed columns up to the flood point," *Chemical Engineering and Technology*, vol. 18, no. 6, pp. 371–379, 1995.
- [5] R. Billet and M. Schultes, "Relationship between pressure drop and mass transfer in two-phase countercurrent flow columns," *Lipi/Fett*, vol. 94, no. 4, pp. 138–144, 1992.
- [6] R. Billet, "Contribution to design and scale-up of packed columns," *Lipi/Fett*, vol. 92, no. 9, pp. 361–370, 1990.
- [7] J. Kuntz and A. Aroonwilas, "Mass-transfer efficiency of a spray column for CO_2 capture by MEA," in *Proceedings of the 9th International Conference on Greenhouse Gas Control Technologies (GHGT '09)*, pp. 205–209, November 2008.
- [8] Z. P. Xu, A. Afacan, and K. T. Chuang, "Predicting mass transfer in packed columns containing structured packings," *Chemical Engineering Research and Design A*, vol. 78, no. 1, pp. 91–98, 2000.
- [9] I. L. Leites, D. A. Sama, and N. Lior, "The theory and practice of energy saving in the chemical industry: some methods for reducing thermodynamic irreversibility in chemical technology processes," *Energy*, vol. 28, no. 1, pp. 55–97, 2003.
- [10] A. Aroonwilas, A. Chakma, P. Tontiwachwuthikul, and A. Veawab, "Mathematical modelling of mass-transfer and hydrodynamics in CO_2 absorbers packed with structured packings," *Chemical Engineering Science*, vol. 58, no. 17, pp. 4037–4053, 2003.



Hindawi

Submit your manuscripts at
<http://www.hindawi.com>

